AN INTEGRAL MODEL FOR POOL SPREADING, VAPORISATION AND DISSOLUTION OF HYDROCARBON MIXTURES

María Isabel Fernandez[2], Mike Harper[2], Haroun Mahgerefteh[1], and Henk W. M. Witlox[2]
[1]Department of Chemical Engineering, University College London
[2]DNV Software, London

A two-phase or liquid release of flammable or toxic fuel may rainout forming a liquid pool. This represents a major safety hazard as the liquid will evaporate upon contact with the substrate forming a flammable vapour cloud. This paper describes a new robust model for spreading, vaporisation and dissolution of a multi-component pool. The new model is an extended version of the pool model PVAP in the Phast consequence modelling package. The multi-component pool model tracks the mixture composition of the transient pool as a function of time, and employs established mixing rules to estimate overall pool properties. Two distinctive cases for pool vaporisation are studied namely boiling and evaporation. Additionally, the model makes continuous checks for transitions between boiling and evaporation by performing a bubble point calculation at each step of the simulation. The present work introduces for the first time a model for the dissolution of water-soluble chemicals present in a multi-component pool. Predictions using the model are compared against the widely-used HGSYSTEM multi-component pool model, LPOOL, and published experimental data in terms of numerical robustness and accuracy.

1. INTRODUCTION

The release of a flammable or toxic fuel, depending on the material's volatility and storage conditions, may rainout forming a liquid pool. This represents a major safety hazard as the liquid will evaporate upon contact with the surface forming a vapour cloud that can disperse into the atmosphere and reach population centres.

Many models are reported in the literature for estimating the vaporisation rate from a liquid pool under different scenarios and with different levels of accuracy with respect to experimental data (Ivings et al., 2009). The pool model PVAP in Phast (Process Hazard Analysis Software Tool) predicts pool spreading, evaporation and dissolution, with good agreement against real data for cryogenic spills such as liquefied methane on land and water surfaces (Witlox, 2006). Webber and Witlox (2003) describe further verification of Phast pool model against the model GASP (Gas Accumulation over a Spreading Pool). Additionally, CFD based models (Ponchaut et al. 2011) have shown good agreement with PVAP in its prediction of the cumulative amount of vapour generation.

For mixtures, the original PVAP model adopts so-called 'pseudo-component' mixture modelling which approximates the behaviour of the multi-component mixture as a pure component using averaged material properties for e.g. boiling temperature, vapour pressure, etc. The current paper describes a new extended and more robust model for spreading, vaporisation and dissolution of a multi-component pool. This model will be referred to in this paper as PVAP-MC and is scheduled to be released in a future version of Phast. PVAP-MC models multi-component pools assuming ideal behaviour according to Raoult's Law in line with the methodology proposed by Cavanaugh (1994).

Chapter 2 describes the underlying theory for PVAP-MC. To account for the mixture behaviour, the MC model tracks the transient pool inventory at each step, and employs established mixing rules to estimate overall pool properties. Two distinctive cases for pool vaporisation are studied: boiling and evaporation. Additionally, the model makes continuous checks for transitions between boiling and evaporation by performing a bubble point calculation at each step of the simulation. The dissolution of water-soluble chemicals present in the mixture is introduced in the present work. This is considered to be a novel feature as compared to existing MC models. Chapter 3 describes the numerical solution. Chapter 4 presents results for PVAP-MC. Section 4.1 summarises the verification of PVAP-MC against the HGSYSTEM multi-component pool model LPOOL (Post, 1994). Section 4.2 describes PVAP-MC validation against published experimental data. Chapter 5 presents the conclusions and further work.

2. THEORY

The extended PVAP multi-component model comprises the following equations: a spreading law to determine the variation of the pool radius as a function of time; a mass balance around the control volume of the pool for each component in the mixture; an energy balance to determine the pool temperature assuming the pool is shallow enough that it can be considered well-mixed.

2.1 POOL SPREADING

The pool spreading law in PVAP-MC is identical to the original PVAP model (Witlox, 2006).

For the spreading of pools on water, the radius r (m) of the pool is expressed as an explicit analytical function of time t (s) for both instantaneous and continuous releases in line with the paper by Dodge et al (1983). Thus the spreading of a pool on water is divided into three consecutive regimes: gravity-inertia, gravity-viscous and viscous-surface tension. In each regime one or more of the forces governing the pool spreading (gravitational, resistive, viscous and surface tension forces) is dominant and subsequently governs the velocity at the edge of the pool. See the Phast 6.7 theory manual for PVAP (Witlox, 2006) for full details.

The spreading law for pools on land follows from Shaw and Briscoe (1980):

$$\frac{dr}{dt} = \sqrt{2g(h - h_{\min})} \qquad (1)$$

where r is the pool radius (m), t is time (s), g is the gravitational constant (m/s^2), h is the pool depth (m) and $h_{\min}$ is the minimum pool depth (m) set equal to the roughness length of the surface.

2.2 CONSERVATION OF POOL MASS AND POOL ENERGY

Figure 1 is a schematic representation of the different heat and mass transfer phenomena which take place in the pool.

The mass balance for the mass of component i, $M_{pool,i}$ (kg), in the pool is given by:

$$\frac{dM_{pool\ i}}{dt} = S_i(t) - E_{vap\ i}(t) - E_{sol\ i}(t) \qquad (2)$$

where $S_i(t)$ is the spill rate (kg/s), $E_{vapi}(t)$ the vaporisation rate (kg/s) and $E_{sol\ i}(t)$ the dissolution rate (kg/s). The sub-index i here and in subsequent symbols refers to component i.

The energy balance is expressed as:

$$\frac{dT_{pool}}{dt}$$

$$= \left[Q_{in} + S(t)c_{p\,spill}\left(T_{spill} - T_{pool}\right) \right.$$

$$\left. - \sum_{i=1}^{n} E_{vap\ i}(t)\,\Delta H_{vap\ i} - \sum_{i=1}^{n} E_{sol\ i}(t)\,\Delta H_{sol\ i} \right] \Bigg/$$

$$c_{p\,pool}\,M_{pool}$$

$$(3)$$

Here, Q_{in} is the sum of the heat contributions from conduction, convection and radiation (W); c_{pspill} and $c_{p\,pool}$ are respectively the specific heat capacity (J/kg/K) at the spill and pool temperatures and compositions; T_{spill} and T_{pool} are the spill and pool temperatures (K); ΔH_{vapi}

and $\Delta H_{sol\ i}$ are respectively the heats of vaporisation and dissolution (J/kg).

2.3 POOL VAPORISATION AND DISSOLUTION

As was mentioned above, two distinctive cases for pool vaporisation are studied: boiling and evaporation. While the pool is boiling the liquid and vapour phases are modelled in equilibrium governed by Raoult's Law. For evaporation, PVAP's pure component model has been extended to account for the diffusion of multiple components into air. Transitions between boiling and evaporation are determined from both a check in the pool temperature and the energy balance. The dissolution of water-soluble chemicals present in the mixture is introduced as a novel feature of pool models.

2.3.1 Boiling Pools

The pool will boil when its temperature is at the bubble point, T_{bubble}, of the mixture, determined from a flash calculation using Raoult's Law (Wallas, 1985). The rate at which heat must be supplied to the pool for it to remain at the bubble point is defined as (Cavanaugh et al., 1994):

$$Q_{bubble} = M_{pool}\, c_{p\,pool}\left(\frac{dT_{bubble}}{dt}\right) \qquad (4)$$

where Q_{bubble} is the rate of heat added to the pool (W).

As the total heat entering the pool is used in both the vaporisation of the liquid and in maintaining the pool at the bubble point (Q_{bubble}), the overall vaporisation rate from a boiling pool is determined by insertion of Equation (4) into the energy balance (3) as:

$$E_{vap}(t)$$

$$= \left[Q_{in} + S(t)c_{p\,spill}\left(T_{spill} - T_{bubble}\right) \right.$$

$$\left. - \sum_{i=1}^{n} E_{sol\ i}(t)\Delta H_{sol\ i}(T_{bubble}) - Q_{bubble} \right] \Bigg/$$

$$\sum_{i=1}^{n} Y_{vap\ i}\,\Delta H_{vap\ i}(T_{bubble})$$

$$(5)$$

where $Y_{vap\ i}$ is the mass fraction of component i in the vaporisation stream.

2.3.2 Non-boiling Pools

The pool temperature will drop below the rising bubble-point temperature when not enough heat is provided by the surroundings to compensate the heat losses by evaporation and dissolution. For a non-boiling pool on land, the total pool evaporation rate is determined from the MacKay and
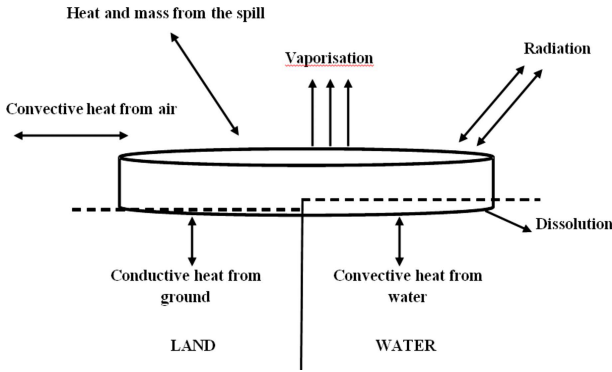
Figure 1. Heat and mass transfer mechanisms between the pool and the surroundings

Matsugu (1973) equation for evaporating pools, extended to mixtures:

$$E_{vap}(t) = \sum_{i=1}^{n} 4.786 \cdot 10^{-3} u_{a(z=10m)}{}^{0.78}$$
$$\times Sc_i^{-0.67} \pi r^{1.89} x_{pool\,i} \frac{M_{c\,i} P_{vap\,i}}{R T_{pool}} \quad (6)$$

Here $u_{a(z=10\,m)}$ is the wind speed measured at 10 m above ground (m/s), $Sc_i = D_{ac\,i}/v_a$ is the Schmidt number, $D_{ac\,i}$ the diffusivity of the component i in air (m²/s), v_a the kinematic viscosity of air (m²/s), $x_{pool\,i}$ the mole fraction in the pool, $M_{c\,i}$ the molecular weight (kg/kmol), $P_{vap\,i}$ the vapour pressure at the pool temperature (Pa) and R the universal gas constant (J/K · kmol)

The total mass evaporated for pools on water is determined from Dodge et al. (1983) model for pure components extended here to mixtures:

$$E_{vap}(t) = (\pi r^2) U_a^* Da_i^* \frac{M_{c\,i} P_v^i}{R T_{pool}} \quad (7)$$

where Da_i^* is the Dalton number for component i as defined in (Witlox, 2006).

2.3.2 Dissolving Pools
The model proposed by Dodge et al. (1983) for the dissolution of pure components from a pool is extended to mixtures:

$$E_{sol}(t) = \sum_{i=1}^{n} 10\pi r^2 U_W^* \rho_W Da_i^* \ln\left(\frac{1}{1 - x_{pool\,i} w_{s\,i}}\right) \quad (8)$$

where U_W^* is the friction velocity of water $= U_a^*(\rho_a/\rho_w)^{1/2}$ (m/s), ρ_a and ρ_w are the air and water densities respectively (kg/m³), Da_i^* is the Dalton number for component i, $w_{s\,i}$ is the molar solubility of component i on water.

2.4 HEAT TRANSFER
As shown in Figure 1, PVAP-MC accounts for heat transfer contributions from the ground or water surface, air and solar radiation. These models in PVAP-MC have not been modified with respect to the original PVAP model. Full details of these can be found in Phast 6.7 PVAP theory manual (Witlox, 2006)

3. NUMERICAL SOLUTION
The pool model comprises a system of ordinary differential equations (ODEs) of the form:

$$\frac{\partial \bar{Y}}{\partial t} = G(\bar{Y}, t) \quad (9)$$

where,

$$\bar{Y} = \begin{pmatrix} r \\ T_{pool} \\ M_{pool}^i \\ M_{vap}^i \\ M_{sol}^i \end{pmatrix} \quad (10)$$

and

$$G = \begin{pmatrix} \begin{cases} Pools\ on\ land = \left[2g\left(\dfrac{\sum_{i=1}^{n} M_{pool}^i}{\pi r^2 \rho_{pool}(T_{pool})} - h_{min} \right) \right]^{0.5} \\ Pools\ on\ water = 0 \end{cases} \\ \dfrac{\sum_{i=1}^{n} S_i(t) c_{p\,spill}(T_{spill} - T_{pool}) + Q_{in} - \sum_{i=1}^{n} E_{vap\,i}(t)\Delta t_{vap}{}^i(T_{pool}) - \sum_{i=1}^{n} E_{sol\,i}(t)\Delta t_{sol}{}^i(T_{pool})}{\sum_{i=1}^{n} M_{pool}^i c_{p\,pool}} \\ S_i(t) - E_{vap\,i}(t) - E_{sol\,i}(t) \\ E_{vap\,i}(t) \\ E_{sol\,i}(t) \end{pmatrix} \quad (11)$$

Here, M_{vap}^i and M_{sol}^i are respectively the cumulative mass vaporised and dissolved (kg). The above equations are: the pool-spreading law (Section 2.1), conservation of mass and energy (Equations (2) and (3), respectively), and equations for the cumulative evaporated and dissolved mass of component i.

The model equations are solved using a public domain numerical solver for ODEs, from Lawrence Livermore National Laboratory (Hindmarsh, 1983). For stiff problems, the ODE solver uses the Backward Differentiation Formula (BDF). This method is a linear multi-step predictor-corrector method. The predictor-corrector process for advancing the solution consists of first generating a predicted value. This value is corrected by iterating over the corrector step until convergence is achieved.

4. RESULTS

First the PVAP-MC results are verified against the pool model LPOOL included in the public-domain hazard-assessment package HGSYSTEM 3.0 (Post, 1994). Secondly they are validated against real data.

4.1 VERIFICATION

PVAP-MC was verified against LPOOL for the case of the spillage of pure methane liquid (at boiling temperature of 111.7K) and a mixture of 50 wt% methane and 50 wt% ethane (at bubble point of 117K). A constant spill rate of 5 kg/s for 120 s was assumed. The following ambient conditions were further selected as PVAP-MC and LPOOL model input: surface roughness length upwind from the pool of 10^{-2} m, wind speed of 1 m/s at 10 m height, neutral stability class D, surface and surrounding air temperature of 288 K and zero solar radiation. The thermal conductivity and diffusivity of the surface were taken as the default values for concrete in LPOOL.

For the first case of a boiling pool of pure methane (at 111.7K), Figure 2 and 3 respectively show the variation of the vaporisation rate and radius, as predicted by PVAP-MC and LPOOL. In both figures good agreement between the predictions of the vaporisation rate and pool radius by PVAP-MC and LPOOL can be observed with maximum deviations of 5%.

For the second case of a methane/ethane pool (at its bubble point), Figure 4 shows the variation of the vaporisation rate with time for the overall mixture and for the individual components. Figure 5 shows the variation of the pool radius with time. From Figure 4 it is observed that the variation of the pool vaporisation rate with time predicted by LPOOL and PVAP-MC follow the same general trend. However, the results of LPOOL present visible oscillations in the region between 5 and 30 s and failed to converge after 2 minutes, while PVAP-MC results follow a smooth curve. The maximum deviations observed between PVAP-MC and LPOOL is 6.5%, this error is considered to be within the range of accuracy required of pool models. In Figure 5 it is observed that the results of the LPOOL and
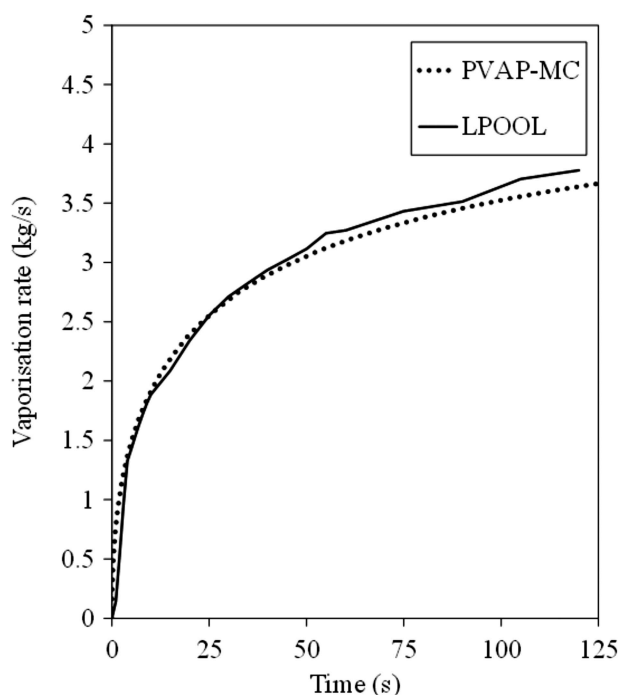

Figure 2. PVAP-MC verification against LPOOL of pool evaporation for methane spill

PVAP-MC simulations are in close agreement with maximum differences of 3%. The bubble point temperature was found to increase with time in both PVAP-MC and
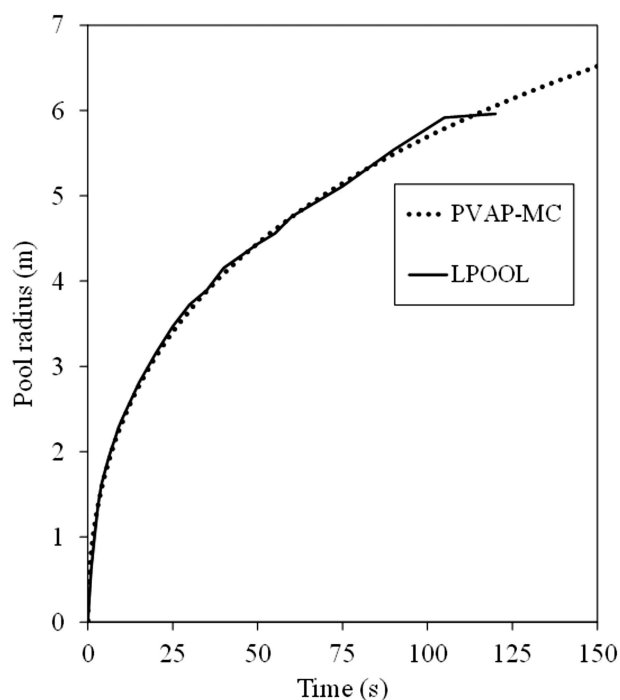

Figure 3. PVAP-MC verification against LPOOL of pool spreading for methane spill
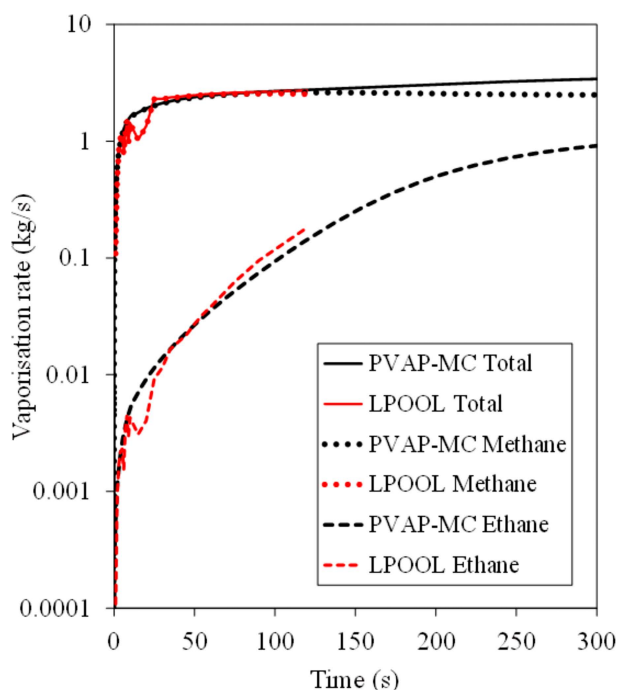
Figure 4. PVAP-MC verification against LPOOL of pool evaporation for methane/ethane mixture
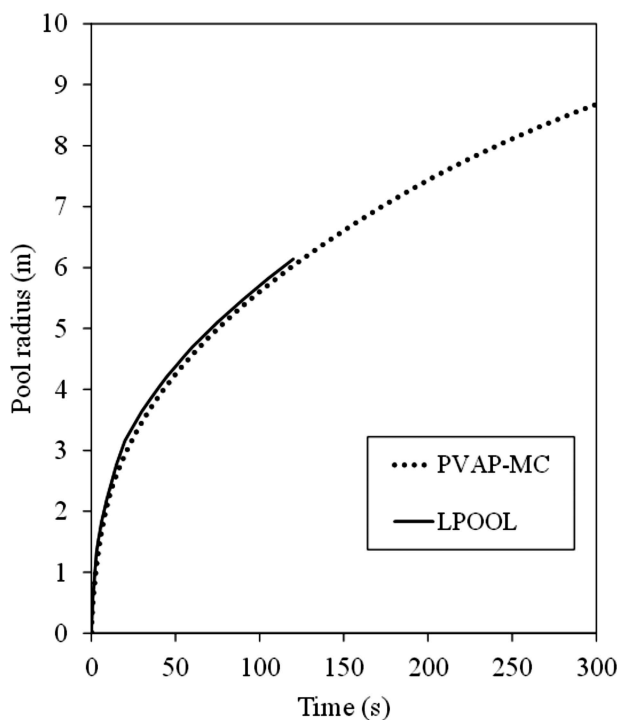

Figure 5. PVAP-MC verification against LPOOL of pool radius for methane/ethane mixture

LPOOL simulations with maximum differences of 3% between both curves.

4.2 VALIDATION

Further assessment of the accuracy of PVAP-MC has been carried out by validation against two experimental data sets of measured pool vaporisation rate involving instantaneous spills on sand (Kawamura and MacKay, 1987) and water (Burgess et al., 1972).

Kawamura and MacKay (1987) measured the evaporation rate of seven volatile chemicals from a circular pan under known meteorological conditions, including summer and winter temperatures. The experiments were conducted at the Environment Canada Atmospheric Environment Services experimental site in Woodbridge, Ontario. Table 1 lists the input data used in PVAP-MC simulations and the average predicted and measured evaporation rates. The average predicted-measured deviation of the four tests is 24.5 %. The best agreement between predicted and measured data is obtained at low vapour pressures and moderate wind speeds (test KM18). However the model is found to be too conservative at low wind speeds (test KM20). At low wind speeds it is possible that vapour accumulates above the pool surface, effectively impeding the mass diffusion through the boundary layer. For simplicity the model assumes the vapour diffuses through a layer of pure air, thus this observation may explain the differences found.

Burgess et al., 1972 conducted a series of experiments conducted for the Bureau of Mines in the 1970′s with LNG spilled on water. The tests were carried out on a 0.074 m² water reservoir, resting on a balance which automatically recorded the weight loss at 50 g intervals. LNG was spilt instantaneously from a tilting container onto the water reservoir from a height of 0.1 and 0.3 m. The total mass vaporised with time was determined from the balance readings. Table 2 shows the release data and prevailing experimental conditions used as input data for the PVAP-MC simulations. Figure 6 compares the variation of the measured mass vaporised against predicted (PVAP-MC) data for a simulation of pure methane and LNG. From Figure 6 good agreement is observed between the LNG predicted data and the measurements with an average deviation of 5%. The results of the methane simulation are less accurate, although conservative, with maximum differences of 10% with respect to the experimental data.

5. CONCLUSIONS AND FUTURE WORK

This paper presented a new robust model PVAP-MC for spreading, vaporisation and dissolution of a multi-component pool. PVAP-MC is an extended version of the pool model PVAP in the Phast consequence modelling package. Two distinctive cases for pool vaporisation were studied namely boiling and evaporation. The present work introduced for the first time a model for the dissolution of water-soluble chemicals present in a multi-component pool.

Table 1. Validation of PVAP-MC) against Kawamura and MacKay (1987) experiments

Spill			Instantaneous	
Pasquill stability class			D- neutral	
Reference height for wind speed (m)			10	
Bund diameter (m)			0.46	
Type of surface			Sand-user defined	
Surface roughness factor			2.6	
Thermal conductivity (W/m.K)			2.08	
Thermal diffusivity (m^2/s)			$7 \cdot 10^{-7}$	
KM18	**KM20**	**KM21**	**KM22**	**Test number**
Toluene	n-Hexane	n-Pentane	n-Pentane	Substance
3.46	2.62	4.37	2.49	Spill mass (kg)
298.15	300.15	296.15	298.15	Spill temperature (K)
872	728	647	861	Solar radiation (W/m^2)
298.15	300.15	296.15	298.15	Atmospheric temperature (K)
2.65	1.59	4.94	5.42	Wind speed (m/s)
298.15	300.15	296.15	298.15	Surface temperature (K)
3.9	7.28	23	27.1	Measured evaporation rate (kg/m^2.h)
4.42	10.31	27.08	33.79	Predicted evaporation rate (kg/m^2.h)
-13%	**-42%**	**-18%**	**-25%**	**Deviation predicted-real data (%)**

The results of the model verification found that PVAP-MC predicts the same trend for the pool results as the HGSYSTEM model LPOOL, and the differences observed are within the range of accuracy required of simple pool models. Nonetheless, the implementation of a robust solver shows a marked improvement on the numerical stability of the results of PVAP-MC as compared to LPOOL. Validation of PVAP-MC against experimental data showed relative good agreement between model predictions and measurements with average errors ranging between 5 and 24%. Future work in this model will include its extension to non-ideal mixtures and the addition of chemical reactions between reactive pools and water. Additionally further model validation against experimental data is recommended, particularly for water soluble chemicals.
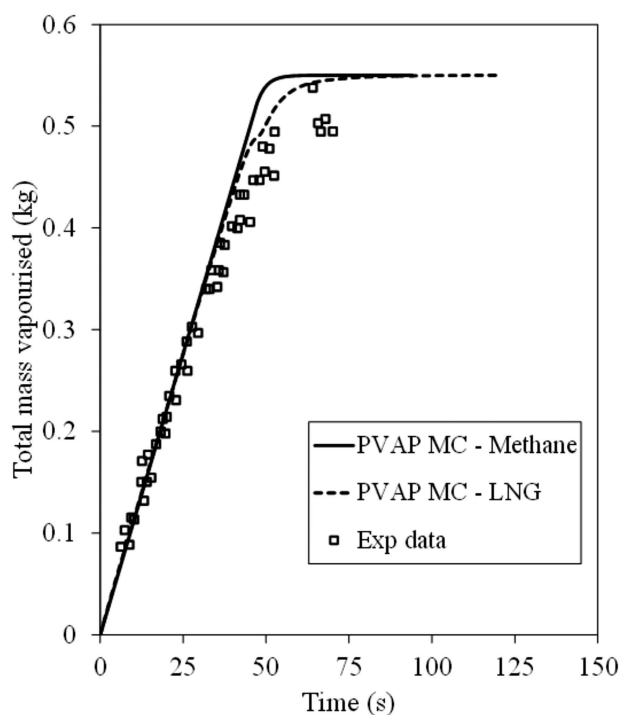
Table 2. Release data and prevailing conditions for Bureau of Mines (Burgess et al., 1972) set of LNG experiments

Spill	Instantaneous
Spill mass (kg)	0.55
Spill temperature (K)	111.66
Surface temperature (K)	278.15
Type of surface	Deep water
Composition LNG (% v/v):	94.74% methane
	5.2% ethane
	0.04% propane
	0.02% n-butane

Figure 6. PVAP-MC validation against Burgess et al. (1972) experiments for total mass of LNG vaporised

NOMENCLATURE

r	=	pool radius (m)
t	=	time (s)
g	=	gravitational constant ($9.8 \ m/s^2$)
h	=	pool depth (m)
h_{min}	=	minimum pool depth (m)
$M_{pool,i}$	=	pool mass for component i (kg)
$S_i(t)$	=	spill rate (kg/s)
$E_{vap}(t)$	=	vaporisation rate (kg/s)
$E_{sol}(t)$	=	dissolution rate (kg/s)
Q_{in}	=	sum of the heat contributions from conduction, convection and radiation (W)
$c_{p \ spill}$	=	specific heat capacity at the spill temperature (T_{spill}) and composition (J/kg/K)
$c_{p \ pool}$	=	specific heat capacity at the pool temperature (T_{pool}) and composition (J/kg/K)
ΔH_{vap}	=	heat of vaporisation (J/kg)
ΔH_{sol}	=	heat of dissolution (J/kg)
Q_{bubble}	=	heat contribution due to the variation in the bubble point temperature (W)
Y_{vap}	=	mass fraction in the pool vaporisation stream
$u_{a(z=10 \ m)}$	=	ambient wind speed measured at 10 m above ground (m/s)
Sc	=	Schmidt number (-)
$D_{ac \ i}$	=	diffusivity of the component i in air (m^2/s)
v_a	=	kinematic viscosity of air (m^2/s)
x_{pool}	=	mole fraction in the pool
M_c	=	molecular weight (kg/kmol)
P_{vap}	=	vapour pressure at the pool temperature (Pa)
R	=	universal gas constant (J/K.kmol)
Da_i^*	=	Dalton number (-)
U_w^*	=	friction velocity of water (m/s)
ρ_a	=	air density (kg/m^3)
ρ_w	=	water density (kg/m^3)
w_s	=	molar solubility
M_{vap}	=	cumulative mass vaporised (kg)
M_{sol}	=	cumulative mass dissolved (kg)

REFERENCES

Cavanaugh II, T., Siegell, J., & Steinberg, K., 1994. Simulation of Vapor Emissions from Liquid Spills. *Journal of Hazardous Materials, 38* (1): 41–63.

Burgess, D., Biordi, J., & Murphy, J., 1972. *Hazards of spillage of LNG into water.* U.S. Bureau of Mines. PMSRC Report No. 4177.

Dodge, F., Park, J., Buckingham, J., & Magott, R., 1983. *Revision and experimental verification of the hazard assesment computer system models for spreading, movement, dissolution, and dissipation of insoluble chemicals spilled onto water.* Washington.

Hindmarsh, A., & Radhakrishnan, K., 1993. *Description and use of LSODE, the Livermore Solver for Ordinary Differential Equations.* California: Lawrence Livermore Laboratory Report.

Ivings, M., Webber, D. M., Gant, S. and Jagger, S. (2009). *LNG source terms models and hazard analysis: a review of the state-of-the-art and approach to model assessment.* Quincy, Massachusets, USA: The Fire Protection Research Foundation.

Kawamura, P., & MacKay, D., 1987. The evaporation of volatile liquids. *Journal of Hazardous Materials*, 15, 343-364.

Leonelli, P., Stramigioli, C., & Spadoni, G., 1994. The modelling of pool vaporization. *Journal of Loss Prevention in the Process Industries, 7* (6), 443–450.

MacKay, D., & Matsugu, R., 1973. Evaporation rates of liquid hydrocarbon spills on land and water. *The Canadian Journal of Chemical Engineering, 51*: 434.

Ponchaut, N. F.; Kytömaa, H. K., Morrison, D. R. and Chernovsky, M. K., 2011. Modelling the vapour source term associated with the spill of LNG into a sump or impoundment area. *Journal of Loss Prevention in the Process Industries, 24*: 870–878.

Post, L. (editor), 1994. *HGSYSTEM 3.0 Technical Reference Manual*. Report No. TNER.94.059, Shell Research Limited, Thornton Research Centre. Chester, England.

Shaw, P., & Briscoe, F.,1980. Spread and evaporation of liquid. *Progress in Energy and Combustion Science, 6* (2): 127–140.

Walas, S. M., 1985. *Phase equilibria in chemical engineering.* London.

Witlox, H., 2006. *PVAP- Theory document.* London: DNV Software (Phast 6.7 Technical Reference Documentation).

Webber, D. and Witlox, H., 2003. *PVAP- Verification document.* London: DNV Software (Phast 6.7 Technical Reference Documentation).